Micro-sized Pore Structure Determination in EPDM Rubbers Using High-Pressure ^{129}Xe NMR Techniques

Kee Sung Han,*[†§] Sarah D. Burton,[⊥§] Eric D. Walter,[⊥] Yongsoon Shin,[†] Wenbin Kuang,[‡] and Kevin L. Simmons*[‡]

[†]Physical and Computational Sciences Directorate, Pacific Northwest National Laboratory, Richland, Washington 99352, United States

[⊥]Environmental Molecular Sciences Laboratory, Pacific Northwest National Laboratory, Richland, Washington 99352, United States

[‡] Energy and Environmental Directorate, Pacific Northwest National Laboratory, Richland, Washington 99352, United States

ABSTRACT: The micro-sized pore parameters, such as pore size and distance between pores in a series of model EPDM rubbers, were determined *in situ* under the pressure of 500 psi using ^{129}Xe nuclear magnetic resonance (NMR) techniques: spin-lattice (T_1) and spin-spin (T_2) relaxation measurements, pulsed-field gradient (PFG) NMR, and 2-dimensional exchange spectroscopy (2D EXSY). The T_1/T_2 (>>1) ratio for the xenon confined in the pores is larger than for non-confined free xenon. This suggests that almost the entire pore surface interacts with xenon atoms like a closed pore. While these pores still connect each other through very narrow diffusion/exchange channels, it is possible to observe the echo decay in PFG-NMR and cross-peaks in 2D EXSY. The results show that both diffusion ($D_{pore} \approx 2.1 \times 10^{-10}$ m^2/s) and exchange (exchange rate, τ_{exch} = a few tens of milliseconds) of xenon between a pore within the material and outer surface are prolonged. The exchange distances (l), which corresponds to the xenon gas penetration depth, were estimated to be 70 – 100 μm based on the measured diffusion coefficients and exchange rate ($1/\tau_{exch}$). NMR diffraction analysis reveals that the pore sizes (a) and the pore distances (b) are on the order of magnitude of micrometers and tens of micrometer while the diffusion coefficients of xenon gas in the diffusion channels (D_{eff}) is about10^{-8} m^2/s. Overall, this study suggests that the pores with a few micrometers and connected through very narrow flowing channels with the length of several tens of micrometers are developed from 70 - 100 μm below the rubber surface. Furthermore, the overall steady-state diffusion of xenon is slower, approximately two orders of magnitudes, than the diffusion in the channel between the pores. The pore and exchange distances correlated with the composition of rubbers showed that the properties of EPDM rubber as a high-pressure gas barrier could be improved by reducing the size of cracks and the depth of gas penetration by the addition of both carbon black and silica fillers.

INTRODUCTION

A widely used commercial polymer, ethylene propylene diene monomer (EPDM) rubbers have various macroscopic properties according to the compounding of plasticizers, fillers, and other additives[1-2] by changing the crosslinking of the polymers.[3] To achieve the goal for design, it requires understanding the microscopic structure and morphology correlated with the macroscopic properties of the polymers. One area of applications, EPDM rubbers, are used as O-rings or containers for handling high-pressure gas, such as hydrogen.[2, 4] When rubbers contact with high-pressure gas, it is possible to penetrate the pressurized gas into the rubber and concentrate gas in pores inside the rubbers.[5] Therefore, understanding pore parameters, such as pore size, pore distance, the gas penetration depth, and the dynamic properties of gas in the rubber and its pores correlated with the compounds of rubbers, will be beneficial for the rational design of the rubbers for the application with high-pressure gas.

Nuclear magnetic resonance (NMR) is a widely used technique for studying the network structure and rubber-filler interactions in EPDM rubbers[1, 3, 6-7] and the interactions of dissolved hydrogen gas with the host substances,[4-5, 8] primarily employing ^{13}C and ^{1}H NMR. However, in this study, we are interested in the pore structure under high pressure. Therefore ^{129}Xe NMR techniques were employed. It has been demonstrated that various ^{129}Xe NMR techniques, such as 2-dimensional exchange spectroscopy (2D EXSY) and pulsed-field gradient (PFG) NMR, are helpful to elucidate the pore structure of the polymers and porous materials. [9-14] In this study, xenon gas was confined in a series of EPDM rubbers (Table S1 in Supporting information) under 500 psi of ^{129}Xe.

Experimental

Sample Preparations. A series of ethylene propylene diene monomer (EPDM) rubbers incorporating various fillers and plasticizers were obtained from Takaishi Industries (JAPAN). The details for the composition of the rubber samples are summarized in Table S1. Xe gas was charged in a 5-mm zirconia WHiMS rotor developed for high-pressure solid-state NMR[15] with a custom-built pressure vessel pressurized to 500 psi (~3.5×10^6 Pa) for 30 minutes. For diffusion measurements using a 5-mm commercial liquid NMR probe, the WHiMS sample rotor was mounted on a custom-built 5 mm shaft to fit the 5-mm liquids NMR sample turbine (see Figure S1 in supporting information).

^{129}Xe 2D EXSY and relaxation measurements. Both ^{129}Xe EXSY and spin-lattice (T_1) and spin-spin (T_2) relaxation time measurements were performed on a 300 MHz solid-state NMR spectrometer (Agilent, USA) equipped with a 5-mm magic angle spinning (MAS) NMR probe at 25 °C. For 2D EXSY, T_1, and T_2 measurements, the vendor-supplied pulse sequence (in VNMRJ, Agilent, USA) EXSY, inversion recovery, and spin-echo were used. The Larmor frequency of ^{129}Xe and 90° pulse length were $2\pi \times 83.35$ rad·MHz and 2.8 μs, respectively. All measurements were performed without sample spinning.

^{129}Xe PFG-NMR experiments. The diffusion coefficients (D) of Xe gas confined within rubber pores were measured by ^{129}Xe pulsed-field gradient (PFG) NMR with the PFG stimulated echo sequence composed of bipolar gradients (Scheme 1) to minimize the artifacts, which may be generated due to the interfacial interactions.[16-21] All PFG-NMR measurements were performed on a 600 MHz NMR spectrometer at a Larmor frequency of ^{129}Xe = $2\pi \times 165.83$ rad·MHz with a 5-mm liquid NMR probe (Doty Scientific, USA); the maximum gradient strength and available minimum gradient step are ~3100 and 0.158 G/cm, respectively. The diffusion coefficient (D) of Xe gas in the rubber pore at 25 °C was determined from the Fourier transformed ^{129}Xe PFG echo signal, S(g) recorded as a function of gradient strength fitted with the Stejskal-Tanner equation, [22]

$$S(g) = S(0)exp\left[-D(\gamma g\delta)^2(\Delta - \frac{\delta}{3})\right] \quad (1)$$

where S(g) and S(0) are the echo heights at the gradient strengths of g and 0, respectively, D is diffusion coefficient, γ is ^{129}Xe gyromagnetic ratio (= $2\pi \times 11.777$ rad·MHz·Tesla^{-1}), Δ is diffusion delay, which is the time interval between the two bipolar gradient pairs, and δ is the gradient length. The ^{129}Xe PFG echo profiles of Xe gas confined in the rubber pores were obtained as a function of gradient strength (g) with 16 or 32 equal steps, and the maximum gradient strength was chosen up to ~14 T/m based on the echo height at the maximum gradient strength. The gradient duration (δ) was fixed at 1 ms. Diffusion delay (Δ) dependent diffusion coefficients, D_{app}(Δ) were measured at Δ = 5, 10, 15, 50, and 100 ms. The 90° pulse length of ^{129}Xe was 8 μs. To increase the signal-to-noise ratio, the signal was accumulated up to 64 scans with a repetition delay of 14 s.

Scheme 1. Bipolar gradient stimulated echo pulsed-field gradient NMR sequence. Δ, δ, and g denote diffusion delay, gradient duration, and gradient strength, respectively. The gradient duration $\delta = 2\delta_b$. In this study, the durations δ_1, δ_b, and δ_2 were 0, 0.5, and 0.5 ms, respectively.

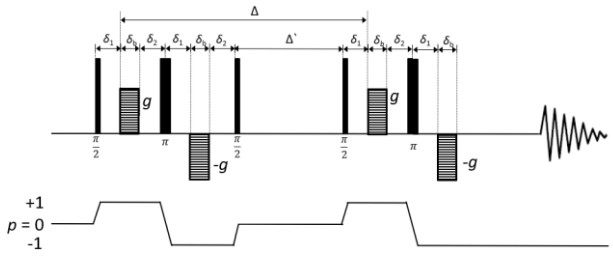

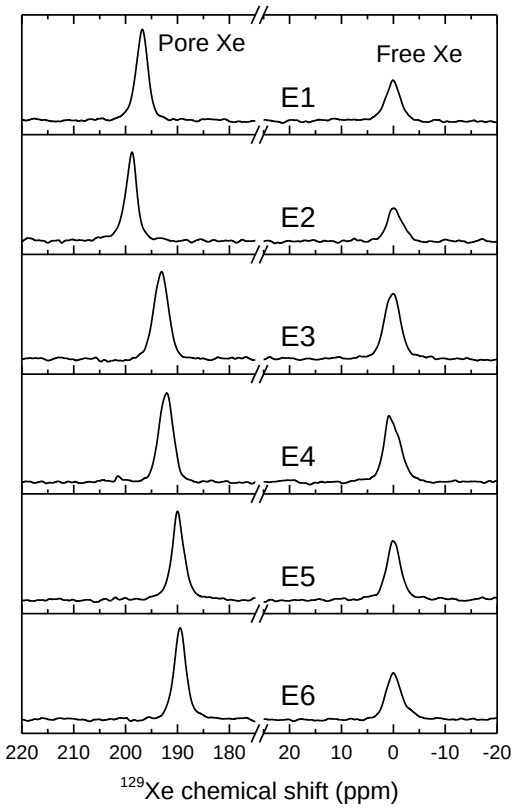

Figure 1. ^{129}Xe NMR spectra obtained from a series of rubbers (E1 - E6) pressurized with 500 psi of Xe gas. The peaks centered at 190 ~199 and 0 ppm come from xenon atoms confined in the pores and residing in the exterior of the rubber pieces, respectively.

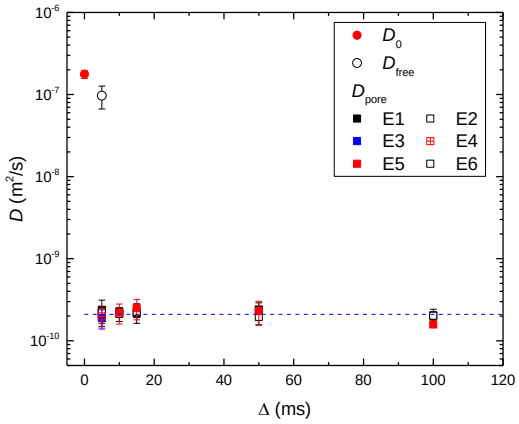

Figure 2. Diffusion coefficients (*D*s) of Xe gas confined in the series of EDPM rubbers determined by ^{129}Xe PFG-NMR.

Table 1. ^{129}Xe spin-lattice (T_1), spin-spin (T_2) relaxation times for pore and free Xe gas and normalized T_2/T_1 ratio for pore; $(T_2/T_1)_{pore}/(T_2/T_1)_{free}$ obtained from free Xe gas and Xe gas located in the pores and the residence time (t_R) of Xe gas in the pore of EPDM rubbers.

Samples	Pore Xe		Free Xe		$(T_2/T_1)_{pore}/(T_2/T_1)_{free}$ (arb. unit)
	$T_{1,pore}$ (s)	$T_{2,pore}$ (ms)	$T_{1,free}$ (s)	$T_{2,free}$ (ms)	
E1	9.65	48.8	11.20	13.2	4.3
E2	8.25	53.1	9.13	16.8	3.5
E3	8.70	36.7	11.00	18.6	2.5
E4	8.89	29.5	8.79	15.6	1.9
E5	9.94	57.5	10.44	20.1	3.0
E6	9.50	50.0	9.30	14.3	3.4

Results and Discussion

In Figure 1, each ^{129}Xe spectra show, two ^{129}Xe resonances centered at the chemical shifts of 190 ~200 (Table S2) and 0 ppm denoted as pore and free Xe, respectively, due to the xenon atoms confined in the rubber pore and those reside in the exterior of the rubber surfaces, i.e., the empty spaces between the rubber pieces.[10, 22] While it is well known that the chemical shift of xenon atoms confined in the pores tends to shift to the higher field (more negative ppm) with the increase of the size of the pore,[23] it can also be shifted due to mobility and composition of the porous material.[24-25] Therefore, it may not be possible to directly correlate the observed ^{129}Xe chemical shifts from pore xenon atoms with the size of the rubber pores. In this study, interestingly, the pore peaks (characteristic peaks of xenon gas trapped in the pores) were gradually shifted to the higher field (lower frequency) with the presence of silica and carbon black while the addition of plasticizer and dioctylsebacate (DOS) reverts the shifts back to the lower field: E2 and E5 compared with E1 and E6, respectively (Table S2); these shifts may also be influenced by the variation of crosslinking.[24-25]

For analysis of the interaction between Xe gas and rubber pore surface, T_1 and T_2 relaxation times for both confined and free Xe gas (Figure 1) were measured for the rubbers (E1 – E6) pressurized with 500 psi of Xe gas and summarized in Table 1. It showed that $T_2 << T_1$ from both free and confined Xe gas for all samples in contrast to bulk fluids for which $T_1 = T_2$ in extreme narrowing limit, $\omega_0\tau_c << 1$, where ω_0 is the Larmor frequency, and τ_c is the rotational correlation time. This behavior in relaxation mechanisms is consistent with the 2-dimensional (2D) relaxation theory incorporating strong interaction between the guest fluids and host solid surfaces with a fast exchange between the guest molecules (those with and without contacting the pore surfaces).[26] The 2D relaxation behavior observed from the cation of ionic liquid confined in mesoporous silica[26] showed that the T_2/T_1 ratios were gradually decreased as the degree of pore filling decreased, i.e., the loading amount of ionic liquid. In that case, as the degree of pore filling decreases, the space between confined ionic liquid and the pore surface generated will become more significant and the confinement effect will be weaker. This weakening of the confinement causes the less efficient exchanges of confined molecules between those with and without contacting the pore surfaces, compared to the exchange which occurs at the interface between ionic liquid and the space,[27] resulting in the smaller T_2/T_1 ratios due to the shorter and longer T_2 and T_1, respectively.[26] Similarly, in this study, the resulting T_2/T_1 ratios are always smaller for free Xe gas compared with those from confined Xe gas: $(T_2/T_1)_{free} << (T_2/T_1)_{pore}$ as a result from $T_{1,pore} \leq T_{1,free}$ and $T_{2,pore} >> T_{2,free}$ due to the presence of the interface at the wall of rotor, and the strong interaction between Xe gas and EPDM rubber.[10] The larger $(T_2/T_1)_{pore}$ compared with the $(T_2/T_1)_{free}$ suggests that the xenon gas is confined very tightly in these rubber pores, and there is no space inside the rubber pores. Then these rubber pores possessing xenon gas can be considered quasi-closed pores connected to each other or to the surface of the rubber with tiny diffusion/exchange channels. If there is no such channel, diffusion and exchange will be prohibited. It is possible to estimate the relative size of the pores across the samples from the T_2/T_1 ratios. Assuming that $T_1 \approx T_2$ for xenon gas filled in the NMR rotor without any rubber pieces, the shorter T_2 compared with T_1 in confinement is due to the surface relaxivity. Therefore, the T_2 relaxation time will be varied according to the contributions of the non-surface contacting (1-s) and surface contacting (s) atoms with the T_2 relaxations, $T_{2,b}$ and $T_{2,s}$, respectively, as follow;

$$\frac{1}{T_2} = \frac{(1-s)}{T_{2,b}} + \frac{s}{T_{2,s}} \quad (2)$$

Here, $T_{2,b}$ can be assumed to be the same as T_1 due to the negligible contribution of the surface relaxivity. Therefore, the T_2/T_1 ratio will be proportional to the size of the pores. For an example, if the pore is extremely large, the T_2/T_1 ratio will be closed to the unity because $T_2 \approx T_1$. For the comparison of the pore sizes across the samples, the $(T_2/T_1)_{pore}$ was normalized with corresponding $(T_2/T_1)_{free}$ because each sample will vary both T_1 and T_2 according to the detailed conditions of the experiment, such as rubber compositions, rubber-to-rotor volume ratio, and errors in pressure. The results summarized in Table 1 (Figure S2 in supporting information) suggesting that the pore sizes will be decreased as following order: E1 > E2 ≥ E6 > E5 > E3 > E4.

Diffusion coefficients of pore and free Xe gas were obtained and presented in Figure 2. Due to the diffusion barrier, the diffusion coefficient will be decreased as the diffusion delay (Δ) increases and then will be reached to the plateau with the steady-state diffusion coefficient, D_∞, when Δ is long enough to get the steady-state diffusion. This diffusion behavior and Δ dependent diffusion coefficients are so-called restricted diffusion and apparent diffusion coefficient, $D_{app}(\Delta)$, respectively. From Δ dependent $D_{app}(\Delta)$, it is possible to estimate the pore structure, such as the radius (d), surface-to-volume ratio (S/V), and tortuosity (T) using equation 3 (or 4), 5, and 6, respectively. [29]

$$f(\Delta) = \left[1 - \frac{D_{app}}{D_0}\right] \cdot \frac{3\sqrt{\pi}}{8\times10^6\sqrt{D_0}} = \frac{1}{d}\sqrt{\Delta}; \text{ open pores} \quad (3)$$

$$D_{app}(\Delta) = \frac{d^2}{20\Delta}; \text{ closed pores} \quad (4)$$

$$D_{app}(\Delta)/D_0 = \left[1 - \frac{4}{9\sqrt{\pi}}\frac{S}{V}\sqrt{D_0\Delta}\right] \quad (5)$$

$$T = \frac{D_0}{D_\infty} \quad (6)$$

All of the above equations contain D_0, which is the diffusion coefficient at Δ = 0 and is thought to be the same as the bulk diffusion coefficient, that is the diffusion coefficient obtained without any

diffusion barriers. In this study, we determined Xe gas diffusion coefficient $D_0 = 1.7\times10^{-7}$ m^2/s, which is in good agreement with previous reports, [10, 14] using 500-psi Xe gas without rubber in the WHiMS sample rotor and plotted at $\Delta = 0$ in Figure 2. Subsequently, we filled the high-pressure sample rotors with rubber pieces ~1 - 2 mm diameter and pressurized the rotor with 500 psi of Xe gas for the diffusion coefficient measurement. The diffusion coefficient (D_{free}) for Xe gas residing outside rubber measured at $\Delta = 5$ ms is $D_{free} = 9.7\times10^{-8}$ m^2/s, which is slightly slower than D_0. Probably this is due to the longer diffusion path resulting from the presence of the rubber pieces. [14] Then, the tortuosity for the Xe gas diffusion through the rubber pieces was estimated to be about 2 from the diffusion ratio $D_0/D_{free} = 1.7\times10^{-7}/9.7\times10^{-8}$. It was not possible to measure the diffusion of free Xe gas when $\Delta > 5$ ms owing to the loss of the echo signal resulting from the fast diffusion and instrumental restrictions (the available minimum gradient step was 0.158 G/cm). As shown in Figure 2, it seems that $D_{free} = 9.7\times10^{-8}$ m^2/s is very close to the steady-state diffusion coefficient due to the larger space between the rubbers with the diameter of 1 ~ 2 mm. For the Xe gas confined in the rubber pores, the diffusion coefficients were determined as $D_{pore} \approx 2.1 \times 10^{-10}$ m^2/s, which decreased three orders of magnitude from D_0 and reached the plateau at $\Delta \approx 5$ ms. This magnitude of decrease is almost the same for all samples. Due to the lack of $D_{app}(\Delta)$ in the early part of Δ, it is hard to estimate the exact pore size using equations 3 because the pore radius can be estimated from the slope of $D_{app}(\Delta)$ vs. $\sqrt{\Delta}$. However, it can give a rough estimation of the size of the rubber pores. Equation 3 shows that the pore radius (d) can be determined from the slope, i.e., from $D_{app}(\Delta)$ plotted as a function of $\sqrt{\Delta}$. The d values calculated from D_0 and D_{pore} at $\Delta = 5$ ms showed that the pore radius would be smaller than ~30 μm. From relaxation analysis, we found that it is possible to consider the pores are a closed pore while it is thought that the pores connect to each other or to the outside of rubber through very tiny narrow channels. Then, we obtained d ~ 4.5 μm at $\Delta = 5$ ms using equation 4. This value is smaller about an order of magnitude than the value obtained using equation 3. Using equation 5, the inverse of surface-to-volume ratio, $(S/V)^{-1}$ (=V/S, volume-to-surface ratio) was estimated to be ≤ 7.5 μm, which corresponds to the sphere with a radius of ≤ 23 μm, which is similar to the pore sizes estimated with equation 3. This is basically because both equations 3 and 5 were derived from the open pores. Suppose it assumes that the sphere with a radius of 4.5 μm, the V/S ratio is estimated to be ~1.5. The tortuosity of materials with similar pore V/S values (several micrometers) are only 3~6 [30], while the estimated tortuosity is ~480 from the D_0/D_{pore} in these rubbers. However, this estimated tortuosity appears too large to be realistic. This may be related to the pore structure, which is thought to be a quasi-closed pore. As observed from the relaxation behavior, the pore can be considered a closed pore with tiny/narrow channels connecting the pores and pores and the rubber surfaces. This means only a tiny amount of Xe gas can diffuse through those channels while most confined Xe gas resides in the pores. Therefore, the apparent diffusion coefficient will be much smaller than the diffusion coefficient of Xe gas diffusing through the channels. Then the tortuosity estimated with the diffusion ratio D_0/D_{pore} will be much larger than the actual tortuosity of the channel. Based on the above observations, it can be concluded that equations 3, 5, and 6, which were developed with an open pore geometry are not able to use for the estimation of the rubber pore structure, such as diameter (d), surface-to-volume ratio (S/V), and tortuosity because the pores are quasi-closed pores.

Table 2. The residence times (t_R) and exchange rates (τ_{exch}) estimated from ^{129}Xe EXSY results and pores sizes (R) and exchange distances between the pores and surfaces in the pore of EPDM rubbers.

Samples (Xe_{pore})	t_R (s)	$(<R^2>)^{1/2}$ (μm)	τ_{exch} (s)	l (μm)
E1	196 ± 22	812 ± 41	15 ± 2	82 ± 4
E2	401± 44	1100 ± 55	22 ± 2	94 ± 5
E3	314 ± 35	944 ± 47	19 ± 2	84 ± 4
E4	125 ± 14	609 ± 31	12 ± 1	68 ± 3
E5	166 ± 18	735 ± 37	14 ± 2	77 ± 4
E6	156 ± 17	727 ± 37	13 ± 2	77 ± 4

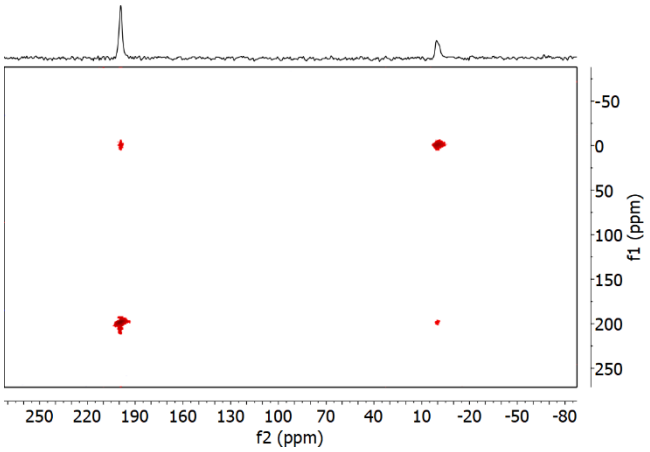

Figure 3. Representative ^{129}Xe 2-dimensional exchange spectrum (2D EXSY) obtained with the mixing time, $\tau_m = 1.2$ s from E2 rubber pressurized with 500 psi of Xe gas.

Due to the discrepancies in the pore sizes estimated from equations 3 and 4, we performed ^{129}Xe 2D EXSY (Figure 3) and estimated the pore size of these rubbers using the intensity ratios between diagonal ($I_{diagonal}$) and cross (I_{cross}) peaks obtained from 2D EXSY in conjunction with spin-lattice relaxation times and diffusion coefficients. From ^{129}Xe 2D EXSY, we observed cross-peaks, as shown in Figure 3, between the two peaks that come from Xe gas confined in the pores and those staying outside of pores (free Xe gas). Then the peak intensities of the cross-peak (I_c) and diagonal peak (I_d) for Xe gas confined in the pores were used to estimate the residence time (t_R) of Xe gas staying in the pore of rubbers using equation 7, which was derived from a two-site exchange model: [9]

$$\frac{I_c}{I_d} = \frac{x_{pore} k \sinh(\alpha t_m)}{\alpha\left[\cosh(\alpha t_m) - \frac{\beta}{\alpha}\sinh(\alpha t_m)\right]} \qquad (7)$$

with $\alpha = \sqrt{\beta^2 + x_{free}x_{pore}k^2}$ and $\beta = \frac{1}{2}\left[(x_{free} - x_{pore})k + \frac{1}{T_{1,pore}} - \frac{1}{T_{1,free}}\right]$,

where x_{pore} and x_{free} are the populations and $T_{1,pore}$ and $T_{1,free}$ are spin-lattice relaxation times of pore confined and free outside Xe gas, respectively. The estimated t_R value, which is the reciprocal of

the k value, is shown in Table 2. Then the mean square radius, $\langle R^2 \rangle$ of the pore can be estimated using equation 8, [9]

$$k = \frac{1}{t_R} = \frac{15D}{\langle R^2 \rangle} \quad (8)$$

For more structure analysis, we used $I_{diagonal}$ and I_{cross} obtained from the peak at ~195 ppm, characteristic of xenon atoms confined in the pores. The results, which are too large to be real, showed that the pore radius, $(\langle R^2 \rangle)^{1/2}$ distribute from 600 to 1100 μm (Table 2), which are comparable with the size (diameters of 1 ~ 2×10^3 μm) of the rubber pieces used for the NMR measurements and larger about two orders of magnitude than those obtained using equation 4. Based on equation 8, the pore size is proportional to the residence time t_R of the Xe gas in the pores. Even though the pore sizes are similar between the open and closed pores, the pore size of closed pore will be estimated larger than that of open pore because the t_R for the gas in the closed pore will be longer than t_R in the open pore. Based on this observation, the pore of these EPDM rubbers can be considered closed pore but with tiny diffusion and exchange channels connecting the pores and the rubber`s surface; otherwise, diffusion and exchange will not be permitted. From the peak intensity ratio between the diagonal (I_d) and cross (I_c) peaks, it is possible to estimate the exchange time, τ_{exch} between the two different sites as shown in equation 9, [31]

$$\tau_{exch} = -\frac{\tau_m}{\ln\left(\frac{I_c - I_d}{I_c}\right)} \quad (9)$$

where τ_m is the mixing time. Then the exchange distance, l between the two sites can be estimated using τ_{exch} in conjunction with the diffusion coefficient, D determined from PFG-NMR using equation 10, [31]

$$D = \frac{l^2}{2d \cdot \tau_{exch}} \quad (10)$$

where d = 1, 2, and 3 for 1, 2, and 3-dimensional diffusions, respectively. We found that Xe gas diffuse to other pores and the rubber surfaces along with tiny diffusion channels. Then it can be considered that the exchange between the confined and free xenon gas may occur through quasi one-dimensional diffusion (d =1) channels. Here, the exchange distance l is closely related to the distance from the pore inside of the rubber to the rubber surface. The sizes (diameters of 1 ~ 2×10^3 μm) of rubber pieces used for the NMR measurements are larger 10 ~ 20 times than the estimated exchange distances distributed from 70 to 100 μm (Table 2), suggesting that the pores confined xenon gas are developed from 70 ~100 μm below the surfaces. As shown in Table 2, the τ_{exch} and l were shorter for free Xe gas than pore Xe gas, probably due to the fast exchange of Xe gas on the surface of the rubber pieces with small open pores.

Based on the above observations, we carefully analyzed the ^{129}Xe PFG-echo profiles and then found an additional diffusion component on an echo decay so-called 'NMR diffraction' as observed previously from ^{129}Xe PFG-NMR performed with Xe gas flowing through glass beads[13] and diffusing in the pores of zeolites.[11] This is probably due to rubber pores connecting each other with tiny diffusion/exchange channels. The ^{129}Xe PFG-echo profile obtained with 32 gradient steps for E5 rubber presented in Figure 4 (Figure S3, supporting information) showed that the echo intensities gradually decreased with an additional oscillatory component. The pattern is not evident probably due to the distributions of pore size and the length of diffusion/exchange channels, i.e., the distance between the pores. [32 33 34 35] In addition, for these rubbers it is thought that there are quasi-closed pores connected to each other through tiny diffusion channels. Xe atoms can diffuse fast through these, suggesting that the smaller amplitude of the oscillatory component in the diffraction pattern may be a result from this tiny contribution of fast diffusing Xe atoms to the PFG-echo profile. Also, it is well known that the diffraction pattern can be varied by the PFG parameters, such as gradient duration and strength, along with the diffusion time,[36] which are closely correlated with the measured diffusion range. The NMR diffraction analysis can give a rough idea for the pore structures.[33, 37-39] Then we fitted it with the NMR-diffraction equation 11,[37]

$$E(q,\Delta) = |s_0(q)|^2 \exp\left[-\frac{6D_{eff}\Delta}{b^2+3\xi^2}\left(1 - \exp(-2\pi^2 q^2 \xi^2)\frac{sin(2\pi qb)}{2\pi qb}\right)\right] \quad (11)$$

where the local structure factor of S_0 is

$$s_0(q) = \frac{sin(\pi qa)}{\pi qa} \quad (12)$$

$q = \gamma\delta g/2\pi$, ξ is the standard deviation of the mean pore distance of b, a is the pore size (radius), D_{eff} is the diffusion coefficient for migration between the pores, and Δ is the diffusion time. The echo profile for E5 rubber fitted with NMR diffraction gave that D_{eff} = $1(\pm1)\times10^{-8}$ m^2/s, a = 3.2 μm, and b = 11 μm. From the NMR diffraction behaviors across the samples, we found that $D_{eff} \approx 1\sim5\times10^{-8}$ m^2/s, a = 3 ~ 5 μm, and b = 5 ~ 27 μm. The results are summarized in Table 3. These results are pretty similar to the observation from the xenon diffusion in the pores of zeolites with the sizes of 6 – 10 μm and 15 – 25 μm, showing that the intra-crystalline diffusion with $D = 6\times10^{-10}$ m^2/s accompanying with fast, long-range diffusion.[11] While there will be some errors in the determination of a, b, and D_{eff} using diffraction behavior due to its blurry, the results can give the range of the pore size, pore distance, and the diffusion coefficient in the channels connecting pore-to-pore and pore-to-surface that revealed as a few micrometers, several tens of micrometers, and ~10^{-8} m^2/s, respectively. These values are in reasonable agreement with the values obtained from the above analysis. For instance, the pore size obtained from equation 4 with the steady-state diffusion coefficients is ~4.5 μm and free Xe gas diffusion coefficient $D_0 = 1.7\times10^{-7}$ m^2/s. Also, the pore sizes determined from NMR diffraction are in good agreement in their order with the relative size of the pores determined from the T_2/T_1 ratios (Figure S4 in supporting information). It is reasonable that the pore distances are smaller than the exchange distances: $b < l$ because the exchange distance, l, is mainly related to the distance from the pore to the surface, while b mainly reflects the distance between the pores that is thought to be shorter than the exchange distance l. Interestingly, it revealed that the pore distances tend to vary inversely with the exchange distances (Figure S5 in supporting information). This suggests that the pore distances tend to be shorter in the pores located in the deeper inside of rubbers and *vice versa*, as shown in Figure 5 and Figure S5. Probably, the exchange distance of Xe gas in these rubbers is closely correlated with the geometry of the pores, such as pore size, shape, and distribution through the material. In Figure S6 (Supporting Information), it is shown that the exchange

distance decreased with the increase of the ratio *b*/*a* and the decrease of *a*. This suggests that the exchange distance will be shorter when the smaller pores are formed farther away from the other pores.

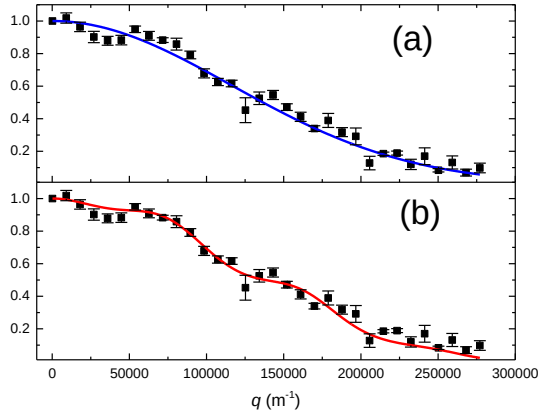

Figure 4. The ^{129}Xe PFG-echo profile obtained from the confined Xe gas in E5 fitted with (a) the Stejskal-Tanner equation, eq (1): $D = 2.0\times10^{-10}$ m^2/s and (b) NMR diffraction equation: $D_{eff} = 1\ (\pm1) \times 10^{-8}$ m^2/s, $a = 3.2$ μm and $b = 11$ μm.

Table 3. The pore size (*a*), pore distance (*b*), and effective diffusion coefficient (D_{eff}) for each rubber obtained from NMR diffraction.

Samples	*a* (μm)	*b* (μm)	D_{eff} (m^2/s)
E1	4.9 ± 0.1	18 ± 2	1 (± 1) × 10^{-7}
E2	4.3 ± 0.8	6 ± 3	5 (± 3) × 10^{-8}
E3	N/A	N/A	N/A
E4	2.8 ± 0.1	24 ± 1	4 (± 2) × 10^{-8}
E5	3.2 ± 0.1	11 ± 1	1 (± 1) × 10^{-8}
E6	3.9 ± 0.2	13 ± 1	8 (± 5) × 10^{-8}

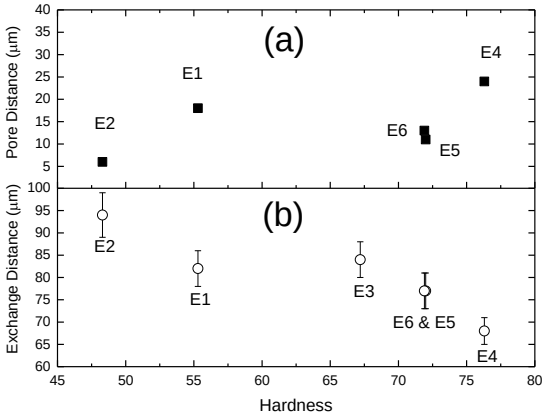

Figure 5. (a) Pore distances and (b) exchange distances potted as a function of the hardness of the rubbers.

Here, it should be emphasized that the pore distance and exchange distance are closely related to the length of the crack and the penetration depth of xenon gas into the rubber, respectively. Then the shorter pore-pore and pore-surface distances will mitigate the formation of the long-range cracks deep inside of the rubber that high-pressure gas can penetrate into, and be better for the storage of high-pressure gas in tanks made of the rubbers. Bear this in mind, we plotted these distance parameters as a function of the hardness of the rubbers (Figure 5) and showing that the pore distance and exchange distance tend to increase and decrease, respectively, with the increase of the hardness of the rubbers. Interestingly, the E5 and E6 rubbers, which added carbon black in addition to silica, showed a relatively shorter pore distance compared with the E4 rubber, which has no carbon black. This suggests that carbon black additive can reduce the size (length) of the crack, probably due to EPDM-carbon filler interfaces. [1, 6] While these rubbers (E5 and E6) showed slightly longer xenon gas penetration depth than the E4 rubber, it is still shorter than the other rubbers (E1, E2, and E3). This confirms that adding both carbon black and silica into EPDM rubber can improve the quality of the rubber as a high-pressure gas container by reducing the length (size) of cracks and the depth of penetration of high-pressure gas into the rubber.

CONCLUSIONS

The pore structures of a series of EPDM rubbers were analyzed using ^{129}Xe NMR techniques, such as relaxation (T_1 and T_2) measurements, PFG-NMR, and 2D EXSY with the rubber samples pressurized with a 500 psi Xe gas. There were two Xe resonances from rubber pore confined and free outside xenon gas at the chemical shifts of ~195 and 0 ppm, respectively. Then it was possible to measure T_1 and T_2 relaxation times and diffusion coefficients for pore confined and free xenon gas separately and estimate the exchange rate ($1/\tau_{exch}$) between pore and free xenon gas utilizing the 2D EXSY experiment. The relaxation ratio, $T_1/T_2 >> 1$ due to the presence of the interaction between xenon atoms and rubbers, is smaller for the xenon atoms confined in the pores compared with free xenon atoms suggesting that the pores are filled with xenon atoms without space between the pore wall and confined xenon atoms like a closed pore. However, due to diffusion/exchange channels inside rubbers, very slow diffusion ($D_{pore} \approx 2.1\times10^{-10}$ m^2/s vs. $D_0 = 1.7\times10^{-7}$ m^2/s of free Xe gas) and exchange ($\tau_{exch} \approx 10 \sim 20$ s) between confined and free xenon atoms were observed. Then we concluded that the quasi-closed pores connected each other with tiny/narrow channels. This is the cause of additional decay in the PFG-echo profile, so-called NMR diffraction, which gave the pore parameters of these rubbers, such as pore size (*a*), pore distance (*b*), and diffusion coefficient (D_{eff}) for xenon atoms diffusing in the channel are several micrometers, a few tens of micrometers, and ~10^{-8} m^2/s, respectively. The exchange distances (*l*), which correspond to the distance from the surface to the pores, were estimated to be 70 – 100 μm. This suggests that the Xe gas pores are developed in 70 – 100 μm from the rubber surface. Overall, the results suggest that the Xe pores with the size of several micrometers connected each other through tiny channels with the length of a few tens of micrometers were developed in 70 - 100 μm from the surface under the pressure of 500 psi. Moreover, the diffusion of Xe gas in the channel is faster, about two orders of magnitudes, than overall steady-state diffusion. Based on the pore and exchange distances obtained from these rubbers (E1 – E6), it can be concluded

that adding both carbon black and silica into EPDM rubber may improve the quality of the rubber as a high-pressure gas device.

ASSOCIATED CONTENT

Supporting Information

The Supporting Information is available free of charge on the ACS Publications website at DOI:
The ^{129}Xe PFG-echo spectra, pore distances plotted vs. exchange distances.

AUTHOR INFORMATION

Corresponding Author

*(K.S.H) E-mail: keesung.han@pnnl.gov
*(K.L.S) E-mail: kl.simmons@pnnl.gov

ORCID

Kee Sung Han: 0000-0002-3535-1818
Sarah D. Burton: 0000-0003-3077-6304
Eric D. Walter: 0000-0003-3644-5514
Yongsoon Shin: 0000-0001-7132-2670
Wenbin Kuang: 0000-0002-6389-7180
Kevin L. Simmons: 0000-0002-2429-6219

Author Contributions

§K.S.H and §S.D.B contributed equally to this work.

Notes

The authors declare no competing financial interests.

ACKNOWLEDGMENT

This work was fully supported by the U.S. Department of Energy (USDOE), Office of Energy Efficiency and Renewable Energy (EERE), Hydrogen and Fuel Cells Technologies Office (HFTO) under Contract Number DE-AC05-76RL01830. NMR measurements were accomplished at the Environmental Molecular Sciences Laboratory, a national scientific user facility supported by the Department of Energy's Office of Biological and Environmental Research and located at Pacific Northwest National Laboratory.

Declaration of interest statement

The views and opinions of the authors expressed herein do not necessarily state or reflect those of the United States Government or any agency thereof. Neither the United States Government nor any agency thereof, nor any of their employees, makes any warranty, expressed or implied, or assumes any legal liability or responsibility for the accuracy, completeness, or usefulness of any information, apparatus, product, or process disclosed or represents that its use would not infringe privately owned rights.

REFERENCES

(1) Litvinov, V. M.; Orza, R. A.; Klüppel, M.; van Duin, M.; Magusin, P. C. M. M. Rubber−Filler Interactions and Network Structure in Relation to Stress−Strain Behavior of Vulcanized, Carbon Black Filled EPDM. *Macromolecules* **2011,** *44*, 4887-4900.

(2) Kuang, W.; Bennett, W. D.; Roosendaal, T. J.; Arey, B. W.; Dohnalkova, A.; Petrossian, G.; Simmons, K. L. In Situ Friction and Wear Behavior of Rubber Materials Incorporating Various Fillers and/or a Plasticizer in High-Pressure Hydrogen. *Tribol. Int.* **2021,** *153*, 106627.

(3) Orza, R. A.; Magusin, P. C. M. M.; Litvinov, V. M.; van Duin, M.; Michels, M. A. J. Mechanism for Peroxide Cross-Linking of EPDM Rubber from MAS ^{13}C NMR Spectroscopy. *Macromolecules* **2009,** *42*, 8914-8924.

(4) Fujiwara, H.; Ono, H.; Nishimura, S. Degradation Behavior of Acrylonitrile Butadiene Rubber after Cyclic High-Pressure Hydrogen Exposure. *Int. J. Hydrog. Energy* **2015,** *40*, 2025-2034.

(5) Simmons, K. L.; Kuang, W.; Burton, S. D.; Arey, B. W.; Shin, Y.; Menon, N. C.; Smith, D. B. H-Mat Hydrogen Compatibility of Polymers and Elastomers. *Int. J. Hydrog. Energy* **2021,** *46*, 12300-12310.

(6) Litvinov, V. M.; Steeman, P. A. M. Epdm−Carbon Black Interactions and the Reinforcement Mechanisms, as Studied by Low-Resolution ^{1}H NMR. *Macromolecules* **1999,** *32*, 8476-8490.

(7) Mitra, S.; Jørgensen, M.; Pedersen, W. B.; Almdal, K.; Banerjee, D. Structural Determination of Ethylene-Propylene-Diene Rubber (EPDM) Containing High Degree of Controlled Long-Chain Branching. *J. Appl. Polymer Sci.* **2009,** *113*, 2962-2972.

(8) Nishimura, S.; Fujiwara, H. Detection of Hydrogen Dissolved in Acrylonitrile Butadiene Rubber by ^{1}H Nuclear Magnetic Resonance. *Chem. Phys. Lett.* **2012,** *522*, 43-45.

(9) Weiland, E.; Springuel-Huet, M.-A.; Nossov, A.; Guenneau, F.; Quoineaud, A.-A.; Gédéon, A. Transport Properties of Catalyst Supports Studied by Pulsed Field Gradient (PFG) and 2D Exchange (EXSY) NMR Spectroscopy. *New J. Chem.* **2016,** *40*, 4447-4454.

(10) Junker, F.; Veeman, W. S. Xenon Self-Diffusion in Organic Polymers by Pulsed Field Gradient NMR Spectroscopy. *Macromolecules* **1998,** *31*, 7010-7013.

(11) Bolt-Westerhoff, J. A.; Datema, K. P.; Nowak, A. K.; Stallmach, F.; Kärger, J. PFG NMR Tracer Exchange Measurements of Xenon in Zeolites. *Magn. Reson. Imaging* **1996,** *14*, 967-969.

(12) Gao, S.; Xu, S.; Wei, Y.; Liu, Z.; Zheng, A.; Wu, P.; Liu, Z. Direct Probing of Heterogeneity for Adsorption and Diffusion within a SAPO-34 Crystal. *Chem. Commun.* **2019,** *55*, 10693-10696.

(13) Mair, R. W.; Rosen, M. S.; Wang, R.; Cory, D. G.; Walsworth, R. L. Diffusion NMR Methods Applied to Xenon Gas for Materials Study. *Magn. Reson. Chem.* **2002,** *40*, S29-S39.

(14) Mair, R. W.; Cory, D. G.; Peled, S.; Tseng, C.-H.; Patz, S.; Walsworth, R. L. Pulsed-Field-Gradient Measurements of Time-Dependent Gas Diffusion. *J. Magn. Reson.* **1998,** *135*, 478-486.

(15) Walter, E. D.; Qi, L.; Chamas, A.; Mehta, H. S.; Sears, J. A.; Scott, S. L.; Hoyt, D. W. Operando MAS NMR Reaction Studies at High Temperatures and Pressures. *J. Phys. Chem. C* **2018,** *122*, 8209-8215.

(16) Zheng, G.; Price, W. S. Suppression of Background Gradients in (B_0 Gradient-Based) NMR Diffusion Experiments. *Concepts Magn. Reson. A* **2007,** *30A*, 261-277.

(17) Sun, P. Z.; Seland, J. G.; Cory, D. Background Gradient Suppression in Pulsed Gradient Stimulated Echo Measurements. *J. Magn. Reson.* **2003,** *161*, 168-173.

(18) Galvosas, P.; Stallmach, F.; Kärger, J. Background Gradient Suppression in Stimulated Echo NMR Diffusion Studies Using Magic Pulsed Field Gradient Ratios. *J. Magn. Reson.* **2004,** *166*, 164-173.

(19) Vasenkov, S.; Galvosas, P.; Geier, O.; Nestle, N.; Stallmach, F.; Kärger, J. Determination of Genuine Diffusivities in Heterogeneous Media Using Stimulated Echo Pulsed Field Gradient NMR. *J. Magn. Reson.* **2001,** *149*, 228-233.

(20) Seland, J. G.; Sørland, G. H.; Zick, K.; Hafskjold, B. Diffusion Measurements at Long Observation Times in the Presence of Spatially Variable Internal Magnetic Field Gradients. *J. Magn. Reson.* **2000,** *146*, 14-19.

(21) Zhong, J.; Kennan, R. P.; Gore, J. C. Effects of Susceptibility Variations on NMR Measurements of Diffusion. *J. Magn. Reson. (1969)* **1991,** *95*, 267-280.

(22) Wu, D. H.; Chen, A. D.; Johnson, C. S. An Improved Diffusion-Ordered Spectroscopy Experiment Incorporating Bipolar-Gradient Pulses. *J. Magn. Reson. A* **1995,** *115*, 260-264.

(23) Terskikh, V. V.; Moudrakovski, I. L.; Breeze, S. R.; Lang, S.; Ratcliffe, C. I.; Ripmeester, J. A.; Sayari, A. A General Correlation for the ^{129}Xe NMR Chemical Shift−Pore Size Relationship in Porous Silica-Based Materials. *Langmuir* **2002,** *18*, 5653-5656.

(24) Springuel-Huet, M. A.; Bonardet, J. L.; Gédéon, A.; Fraissard, J. ^{129}Xe NMR for Studying Surface Heterogeneity: Well-Known Facts and New Findings. *Langmuir* **1997,** *13*, 1229-1236.

(25) Sperling-Ischinsky, K.; Veeman, W. S. ^{129}Xe-NMR of Carbon Black Filled Elastomers. *J. Braz. Chem. Soc.* **1999,** *10*, 299-306.

(26) Han, K. S.; Wang, X.; Dai, S.; Hagaman, E. W. Distribution of 1-Butyl-3-Methylimidazolium Bistrifluoromethylsulfonimide in Mesoporous Silica as a Function of Pore Filling. *J. Phys. Chem. C* **2013,** *117*, 15754-15762.

(27) Mattea, C.; Kimmich, R.; Ardelean, I.; Wonorahardjo, S.; Farrher, G. Molecular Exchange Dynamics in Partially Filled Microscale and Nanoscale Pores of Silica Glasses Studied by Field-Cycling Nuclear Magnetic Resonance Relaxometry. *J. Chem. Phys.* **2004,** *121*, 10648-10656.

(28) Ardelean, I.; Mattea, C.; Farrher, G.; Wonorahardjo, S.; Kimmich, R. Nuclear Magnetic Resonance Study of the Vapor Phase Contribution to Diffusion in Nanoporous Glasses Partially Filled with Water and Cyclohexane. *J. Chem. Phys.* **2003,** *119*, 10358-10362.

(29) Palmas, P.; Botzanowski, T.; Guerain, M.; Forzy, A.; Bruneton, E.; Delrio, G. Size Determination of Porosity Inclusions in an Organic Solid Material by ^{1}H NMR Diffusion and SEM-FIB Experiments: The TATB Case. *J. Phys. Chem. B* **2016,** *120*, 4152-4159.

(30) Hurlimann, M. D.; Helmer, K. G.; Latour, L. L.; Sotak, C. H. Restricted Diffusion in Sedimentary Rocks. Determination of Surface-Area-to-Volume Ratio and Surface Relaxivity. *J. Magn. Reson. A* **1994,** *111*, 169-178.

(31) Bottke, P.; Freude, D.; Wilkening, M. Ultraslow Li Exchange Processes in Diamagnetic Li_2ZrO_3 as Monitored by EXSY NMR. *J. Phys. Chem. C* **2013,** *117*, 8114-8119.

(32) Park, S. K.; Han, K. S.; Lee, J. H.; Murugesan, V.; Lee, S. H.; Koo, C. M.; Lee, J. S.; Mueller, K. T. Evolution of Ion−Ion Interactions and Structures in Smectic Ionic Liquid Crystals. *J. Phys. Chem. C* **2019,** *123*, 20547-20557.

(33) Hayamizu, K.; Akiba, E.; Price, W. S. Ion Diffusion Restricted by Time-Dependent Barriers in a Viscous Polyethylene-Based Liquid Electrolyte. *Macromolecules* **2003,** *36*, 8596-8598.

(34) Kuntz, J.-F.; Palmas, P.; Canet, D. Diffusive Diffraction Measurements in Porous Media: Effect of Structural Disorder and Internal Magnetic Field Gradients. *J. Magn. Reson.* **2007,** *188*, 322-329.

(35) Yadav, N. N.; Price, W. S. Impediments to the Accurate Structural Characterisation of a Highly Concentrated Emulsion Studied Using Nmr Diffusion Diffraction. *J. Colloid Interface Sci.* **2009,** *338*, 163-168.

(36) Bar-Shir, A.; Avram, L.; Özarslan, E.; Basser, P. J.; Cohen, Y. The Effect of the Diffusion Time and Pulse Gradient Duration Ratio on the Diffraction Pattern and the Structural Information Estimated from Q-Space Diffusion MR: Experiments and Simulations. *J. Magn. Reson.* **2008,** *194*, 230-236.

(37) Callaghan, P. T.; Coy, A.; MacGowan, D.; Packer, K. J.; Zelaya, F. O. Diffraction-Like Effects in NMR Diffusion Studies of Fluids in Porous Solids. *Nature* **1991,** *351*, 467-469.

(38) Hayamizu, K.; Akiba, E.; Bando, T.; Aihara, Y.; Price, W. S. Nmr Studies on Poly(Ethylene Oxide)-Based Polymer Electrolytes with Different Cross-Linking Doped with $LiN(SO_2cCF_3)_2$. Restricted Diffusion of the Polymer and Lithium Ion and Time-Dependent Diffusion of the Anion. *Macromolecules* **2003,** *36*, 2785-2792.

(39) Saito, Y.; Umecky, T.; Niwa, J.; Sakai, T.; Maeda, S. Existing Condition and Migration Property of Ions in Lithium Electrolytes with Ionic Liquid Solvent. *J. Phys. Chem. B* **2007,** *111*, 11794-11802.

TOC graph

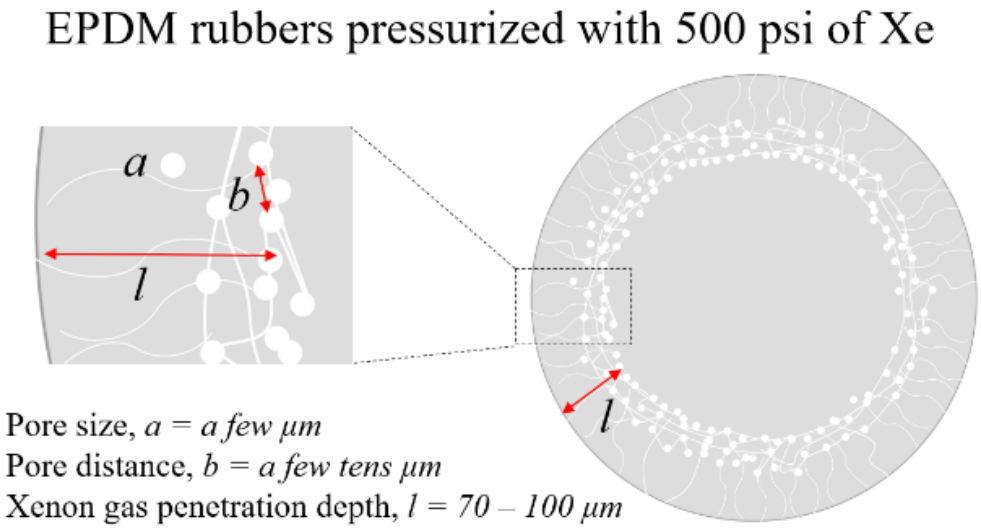
EPDM rubbers pressurized with 500 psi of Xe
a
b
l
l
Pore size, a = a few μm
Pore distance, b = a few tens μm
Xenon gas penetration depth, l = 70 – 100 μm